

Response of a natural phytoplankton community from the Qingdao coast (Yellow Sea, China) to variable CO₂ levels over a short-term incubation experiment

Haimanti Biswas^{1,*}, Jin Jie², Ying Li³, Guosen Zhang³, Zhuo-Yi Zhu³, Ying Wu³, Guo-Ling Zhang², Yan-Wei Li², Su Mei Liu² and Jing Zhang³

¹CSIR-National Institute of Oceanography, Regional Centre, 176 Lawson's Bay Colony, Visakhapatnam 530 017, India

²Key Laboratory of Marine Chemistry Theory and Technology Ministry of Education, Ocean University of China, 238 Songling Road, Qingdao, 266100, P.R. China

³State Key Laboratory of Estuarine and Coastal Research, East China Normal University, 3663 Zhongshan Road North Shanghai 200062, China

Since marine phytoplankton play a vital role in stabilizing earth's climate by removing significant amount of atmospheric CO₂, their responses to increasing CO₂ levels are indeed vital to address. The responses of a natural phytoplankton community from the Qingdao coast (NW Yellow Sea, China) was studied under different CO₂ levels in microcosms. HPLC pigment analysis revealed the presence of diatoms as a dominant microalgal group; however, members of chlorophytes, prasinophytes, cryptophytes and cyanophytes were also present. $\delta^{13}\text{C}_{\text{POM}}$ values indicated that the phytoplankton community probably utilized bicarbonate ions as dissolved inorganic carbon source through a carbon concentration mechanism (CCM) under low CO₂ levels, and diffusive CO₂ uptake increased upon the increase of external CO₂ levels. Although, considerable increase in phytoplankton biomass was noticed in all CO₂ treatments, CO₂-induced effects were absent. Higher net nitrogen uptake under low CO₂ levels could be related to the synthesis of CCM components. Flow cytometry analysis showed slight reduction in the abundance of *Synechococcus* and pico-eukaryotes under the high CO₂ treatments. Diatoms did not show any negative impact in response to increasing CO₂ levels; however, chlorophytes revealed a reverse trend. Heterotrophic bacterial count enhanced with increasing CO₂ levels and indicated higher abundance of labile organic carbon. Thus, the present study indicates that any change in dissolved CO₂ concentrations in this area may affect phytoplankton physiology and community structure and needs further long-term study.

Keywords: Diatoms, increasing CO₂ levels, light stress phytoplankton community, phytoplankton pigment, Qingdao coast.

As a consequence of huge amount of CO₂ release, atmospheric CO₂ concentration is increasing in an alarming rate¹ and also dissolving into the surface ocean

causing significant changes in carbonate chemistry (increasing hydrogen ion concentrations, dissolved CO₂ and bicarbonate ions, and decreasing carbonate ion concentrations and pH; a process known as 'ocean acidification')^{2,3}. Increasing CO₂ levels in seawater may potentially affect marine phytoplankton communities⁴⁻⁶. Noticeable impacts of increasing CO₂ levels on phytoplankton primary production^{7,8} and community composition⁹⁻¹¹ have been clearly documented in several experiments and the responses were highly diverse. Presumably, the observed differential behaviour of diverse groups of marine phytoplankton in response to increasing CO₂ levels is principally because of their dissimilar carbon metabolism patterns¹². Hence, in general, how marine phytoplankton would respond to ongoing increasing CO₂ levels needs to be addressed and requires extensive area-specific studies.

Coastal waters can show high level of variability in CO₂ partial pressure and pH, and hence coastal phytoplankton communities can be less vulnerable to ocean acidification. Virtually, the responses of phytoplankton communities from Qingdao coastal waters to increasing CO₂ levels have not been studied so far. The present short-term study discusses the effects of different CO₂ levels on the natural phytoplankton assemblage from the coastal waters of Qingdao (NW Yellow Sea, China). Although, the short-term incubation experiment may not show any long-term changes in the study area, it can show the responses of the plankton communities over a short-term natural change.

Materials and methods

Study site, water sample collection and experimental settings

Qingdao coast is a part of Yellow Sea (NW) and one of the important marginal seas located between mainland China and the Korean peninsula (Figure 1). This area

*For correspondence. (e-mail: haimanti.biswas@nio.org)

derives its name from the colour of the silt-laden water discharged into it by major Chinese rivers, including the Yellow River, which flows into the Bohai, and the Yangtze. Surface sea water was collected (through a 200 μm mesh to remove large mesozooplankton) with the help of a mechanized boat from the Qingdao coast in three 20 l acid-cleaned carboys and brought back to the laboratory for further experiments. The carboys were kept at 20°C under natural sunlight (10 : 14 h day–night period) for one complete day to let the plankton community to acclimatize. pCO_2 was calculated using dissolved inorganic carbon (DIC) and total alkalinity (TA) following the methodology of Lewis and Wallace¹³. All carbon chemistry parameters (pCO_2 , DIC, TA, pH) were measured in order to calculate the initial pCO_2 in the ambient waters, which was $\approx 460 \mu\text{atm}$. Keeping this CO_2 level as control (in triplicate), two additional higher pCO_2 levels (≈ 640 and $\approx 730 \mu\text{atm}$) were set in triplicate by adding sodium bicarbonate followed by diluted HCl¹⁴. The final pH values of three different pCO_2 levels were 7.99 ± 0.008 , 7.88 ± 0.008 and 7.83 ± 0.001 respectively.

After adjusting the pCO_2 levels in 51 transparent polyethylene containers without any headspace, the bottles were tightly closed with a sealed lock and incubated in triplicate in the same place where the carboys were kept initially in similar conditions for the next 5 days under natural day–night period. Additional care was taken to avoid in/out gassing by wrapping the sealed lock with a parafilm strip. Sampling was done on the sixth day of incubation. Each bottle was mixed gently everyday at a particular time (at 10 am) in order to avoid biomass settlement at the bottom.

Sample analysis

DIC was analysed using the Apollo SciTech's AC-C2 DIC analyzer fitted with a Li-Cor 6262 CO_2 analyzer and

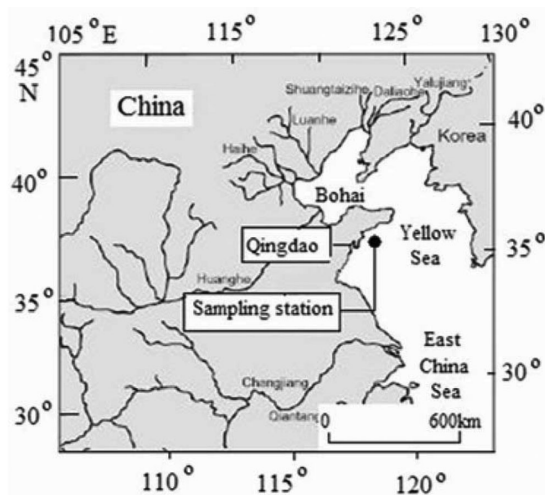


Figure 1. Map showing sampling station in the Qingdao coast, Yellow Sea, China.

Certified Standard Reference Materials (CRMs by Dickson *et al.*¹⁵). Total alkalinity was measured according to Dickson *et al.*¹⁵ using a 794 Basic Titrino (Metrohm). Major nutrients (dissolved inorganic nitrogen (DIN), dissolved inorganic phosphate (DIP) and silicate (Si)) were analysed colorimetrically with the help of an auto-analyzer (San + Analyzer; Skalar Analytical, The Netherlands) following the standard protocol of sea-water analysis^{16,17}.

For phytoplankton pigment analysis, 1 litre of sample water was filtered using GF/F (47 mm) filters and were cut into pieces, added with methanol, ground and phytoplankton pigment was extracted by an ultrasonicator (VCX644, Sonics and Materials, USA) in an ice-bath. Samples were then centrifuged (3000 rpm) and filtered through clean 0.45 μm PTFE membrane. They were analysed using the HPLC system, Agilent 1100 series following the methodology of Zapata and Garrido¹⁸, and Zapata *et al.*¹⁹. Pigments were quantified based on the comparison of retention time and spectra with authentic standards (chlorophyll *a* (chl *a*) and β -carotene were purchased from Sigma-Aldrich Company, USA. The rest 18 standards were purchased from DHI Company).

For particulate organic carbon (POC) and particulate organic nitrogen (PON), 500 ml water sample was filtered using a pre-combusted GF/F 47 mm filter and the filter was dried at 40°C overnight (inside a hot-air oven) and exposed to HCl fume to avoid interference of particulate inorganic carbon (PIC) if any. POC and PON were measured using a mass spectrometer (model: Delta plus XP) connected with a Flash Elemental Analyzer. Urea and potassium nitrate (IAEA) were used as the working standard and black carbon as the reference. Carbon and nitrogen stable isotope ratios ($\delta^{13}\text{C}$ and $\delta^{15}\text{N}$) of particulate organic matter (POM) was measured with the help of an isotopic ratio mass spectrometer (model: Delta plus XP) using PDB as a standard and calculated using the following formula

$$\delta^{13}\text{C}_{\text{POM}} = \left[\left\{ \frac{(^{13}\text{C}/^{12}\text{C})_{\text{sample}}}{(^{13}\text{C}/^{12}\text{C})_{\text{standard}}} \right\} - 1 \right] \times 1000,$$

and

$$\delta^{15}\text{N}_{\text{POM}} = \left[\left\{ \frac{(^{15}\text{N}/^{14}\text{N})_{\text{sample}}}{(^{15}\text{N}/^{14}\text{N})_{\text{standard}}} \right\} - 1 \right] \times 1000.$$

Particulate organic phosphate (POP) was estimated using the method described Aspila *et al.*²⁰. For dissolved organic carbon (DOC) analysis, 40 ml of sea water was filtered through a 0.45 μm filter fitted with a clean syringe and collected in acid-clean brown glass bottles and kept frozen at -20°C till further analysis. Later DOC was determined by high temperature catalytic oxidation with a Shimadzu 5000(A) TOC analyzer. The uncertainty of the concentration range is 2% for the instruments. The instrument blank (5–10 μM) was subtracted from all measured values. Autotrophic pico-plankton, *Synechococcus* and heterotrophic bacteria were analysed with a three-colour

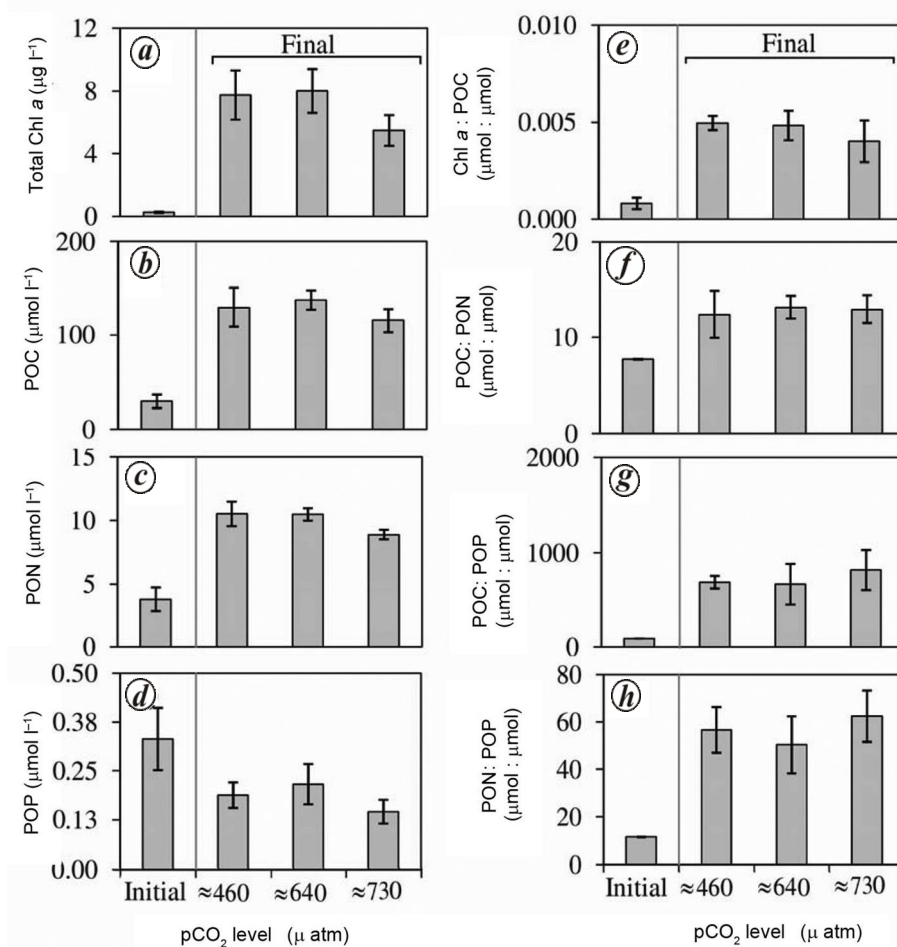


Figure 2. Initial day and final day values of (a) total Chlorophyll *a* (Chl *a*); (b) particulate organic carbon (POC); (c) particulate organic nitrogen (PON); (d) particulate organic phosphate (POP), and the ratios (e) of Chlorophyll *a* to POC; (f) POC to PON; (g) POC to POP and (h) PON to POP under different CO₂ levels (Average \pm SD, $n = 3$; the grey line in each figure separates the initial and final day values of each parameter.)

FACScan™ bench flow cytometer (Becton Dickinson, San Jose, CA USA) equipped with an air-cooled argon ion laser providing 15 mW at 488 nm. Triplicate measurements were made for each sample with precision higher than 7.2% (relative standard deviation). Paired *t*-test was conducted to show the level of significance, in any observed difference between the control and high CO₂ treatments.

Results

Biomass production, elemental composition, dissolved constituents and nutrient uptake

A considerable increase in phytoplankton biomass (both Chl *a* and POC) was observed in all treatments (Figure 2 *b–d*) with a concomitant decrease in all dissolved inorganic nutrients (Table 1) and POP (Figure 2 *d*). DIC concentration decreased <4.5% on average for all treatments (Table 2). However, biomass build-up did not show any significant CO₂-induced effect. The ratios of Chl *a* to

POC (Figure 2 *e*) increased 5.65 times and showed a decreasing trend with increasing CO₂ levels; however, it was statistically insignificant ($P > 0.1$). The initial ratios of POC : PON (Figure 2 *f*), POC : POP ratio (Figure 2 *g*) and PON : POP (Figure 2 *h*) increased considerably in the final samples.

DOC concentrations (initial value was $127.67 \pm 2.42 \mu\text{M}$) showed very small change over the experiment ($125.65 \pm 2.6 \mu\text{M}$; Table 1) and no clear CO₂ effect was observed. Net uptake of DIC from each CO₂ treatment (Table 2) revealed that DIC uptake was 4.83%, 3.73% and 3.22% of the initial DIC values in control, 640 and 730 μatm pCO₂ treatments respectively. Interestingly, the net build-up of POC + DOC (final values of POC + DOC were deducted from the initial values) revealed a poor correlation with net DIC uptake in the high CO₂ treatments. In control, net DIC uptake and POC + DOC build-up values was very close with only 2.13% deviation, whereas, for two high CO₂ treatments these values deviated by 27.12% and 22.12% respectively (Table 2).

Table 1. Initial and final day concentrations of dissolved inorganic nutrients (DIN, DIP and silicate), DOC, POC, PON, POP) in different pCO₂ treatments (DIN = NO₃ + NO₂ + NH₄). ΔSi : N is the consumption ratio calculated by dividing the net Si uptake by net DIN uptake. Values given are average (± SD) and *n* = 3. The reported pCO₂ values are of the initial day

| | | Initial | | | Final | |
|----------------------|---|-------------------------|-------------|-----------------|-------------|-------------|
| Dissolved fraction | ↑ | pCO ₂ (μatm) | | ≈ 460 (control) | ≈ 640 | ≈ 730 |
| | | DIN (μM) | 17.2 ± 2.07 | 4.46 ± 1.4 | 6.45 ± 1.65 | 5.71 ± 0.46 |
| | | Silicate (μM) | 5.92 ± 0.41 | 2.23 ± 0.07 | 2.04 ± 0.17 | 2.14 ± 0.23 |
| | | DIP (μM) | 0.52 ± 0.13 | 0.02 ± 0.01 | 0.01 ± 0.01 | 0.02 ± 0.01 |
| | | DIN : DIP | 33.7 ± 5.5 | 318 ± 222 | 542 ± 142 | 342 ± 236 |
| | | N : Si | 2.9 ± 0.15 | 2.01 ± 0.67 | 3.71 ± 0.49 | 2.68 ± 0.2 |
| | | ΔSi : N | – | 0.75 ± 0.12 | 1.03 ± 0.17 | 0.83 ± 0.02 |
| Particulate fraction | ↑ | DOC (μM) | 125 ± 2.6 | 127 ± 4 | 142 ± 26 | 130 ± 1.7 |
| | ↓ | POC (μM) | 59.1 ± 14 | 130 ± 21 | 138 ± 10.18 | 116 ± 12.71 |
| | | PON (μM) | 7.64 ± 1.9 | 10.5 ± 1.0 | 10.5 ± 0.5 | 8.9 ± 0.41 |
| | | POP (μM) | 0.33 ± 0.08 | 0.19 ± 0.03 | 0.21 ± 0.05 | 0.15 ± 0.03 |
| | | POC : PON | 7.7 ± 0.1 | 12.5 ± 2.5 | 13.2 ± 1.2 | 13.2 ± 1.5 |
| | | POC : POP | 178.3 ± 0.4 | 691 ± 65 | 672 ± 213 | 820 ± 210 |
| | | PON : POP | 23 ± 0.1 | 56.7 ± 9.6 | 50.4 ± 12.1 | 62.5 ± 10.8 |

Table 2. Net DIC uptake, net growth of POC + DOC, percentage change in DIC and percentage deviation between POC + DOC build-up and DIC uptake for different CO₂ levels during the experimental period

| Initial pCO ₂ levels (μatm) | Net change in DIC (μmol l ⁻¹) | Net production of POC + DOC over the experimental period (μmol l ⁻¹) | Percentage change in DIC | Percentage deviation between POC + DOC and DIC uptake |
|--|---|--|--------------------------|---|
| ≈ 460 (control) | 99.87 ± 3.8 | 102 ± 18.02 | 4.83 ± 0.19 | 2.13 |
| ≈ 640 | 83.88 ± 7.9 | 115 ± 17.66 | 3.73 ± 0.41 | 27.12 |
| ≈ 730 | 70.77 ± 2.91 | 91 ± 12 | 3.22 ± 0.13 | 22.12 |

The amount of net nutrient uptake was calculated by subtracting the final concentrations from their initial values and has been presented in Figure 3 *a–c*. The net DIN uptake in the untreated controls was almost 21% higher relative to the high CO₂-treated cells (Figure 3 *a*; *t* = 2.17, *df* = 7, *P* < 0.10). Conversely, net uptake of Si and DIP (Figure 3 *b* and *c*) did not show any significant difference within different CO₂ levels. However, the Si : N and N : P uptake rates were significantly higher at the elevated CO₂ levels (Figure 3 *d* and *f*; *df* = 7, *P* < 0.05). The Si : P uptake rates (Figure 3 *e*) did not show any significant difference between the treatments.

δ¹³C and δ¹⁵N of particulate organic matter

$\delta^{13}\text{C}_{\text{POM}}$ in the untreated controls was changed ($-22.7 \pm 0.2\text{‰}$) by 0.3‰ from its initial value ($-22.3 \pm 0.08\text{‰}$) (Figure 4 *a*). A significant negative linear correlation (*P* < 0.001) was observed between the $\delta^{13}\text{C}_{\text{POM}}$ values and CO₂ levels (Figure 4 *b*; *t* = 5.37, *df* = 7, *P* < 0.002). The average value of $\delta^{15}\text{N}_{\text{POM}}$ (Figure 4 *c*) on the final day (3.1‰) was almost 15 times higher than that on the initial day (0.2‰), indicating high rate of nitrate uptake, which is consistent with the depleted values of DIN on the final day. The average value of $\delta^{15}\text{N}_{\text{POM}}$ in the

controls was 1.2 times higher than that of high CO₂ incubated cells, indicating relatively higher nitrate uptake in the controls which was consistent with the net DIN uptake.

HPLC pigment analysis

Phytoplankton community structure was examined by HPLC and flow cytometry. Fucoxanthin (Fuco), the marker pigment of diatoms was the major contributor among all other pigments. Initial Fuco/Chl *a* ratio was 1 : 1 and remained unchanged in the untreated controls. Fuco/Chl *a* increased by 1.29 times in the high CO₂ treatments (Figure 5 *a*; significant at 95% confidence level; *t* = 2.20, *df* = 7, *P* < 0.05). Diadinoxanthin (DD) and diatoxanthin (DT) were also detected from the cell extracts. DT index [DT/(DT + DD)] was high in the untreated controls and decreased in the high CO₂ treated cells (Figure 5 *b*; *t* = 2.44, *df* = 7, *P* < 0.05).

Most of the pigments usually present in the members of chlorophyta, namely lutein (Lut), chlorophyll *b* (Chl *b*), violoxanthin (Viol), neoxanthin (Neo), antheraxanthin (Anth) and zeaxanthin (Zea) were also detected from HPLC analysis, but their concentrations were much lower relative to Fuco concentration. However, the quantity

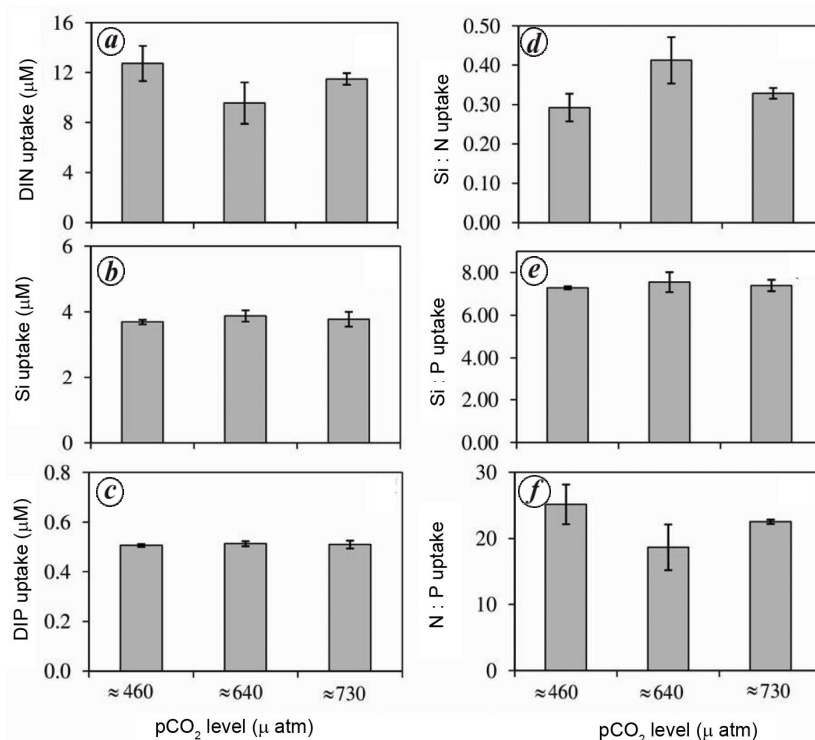


Figure 3. Net uptake of (a) DIN, (b) Si, (c) DIP and the ratios of net uptake of (d) Si : N, (e) Si:P and (f) N : P under different CO₂ levels over the experimental range (average \pm SD, $n = 3$).

and distribution of these pigments showed considerable variation in relation to increasing CO₂ levels. All representative pigments of chlorophyta showed a clear decreasing trend with increasing CO₂ levels. The values of Lut/Chl *a* (Figure 5c), Chl *b*/Chl *a* (Figure 5d) and Neo/Chl *a* (Figure 5e) significantly reduced under elevated CO₂ levels than those of the control ($P < 0.05$). Lut, the marker pigment of the group chlorophyta and Lut/Chl *a* ratio revealed a significant linear negative correlation ($P < 0.01$) with increasing CO₂ levels (Figure 5c), indicating decreased abundance of the members of Chlorophyta under the elevated CO₂ levels. On the contrary, Viol/Chl *a* ratio showed a significant negative linear correlation ($P < 0.01$) with increasing CO₂ levels (Figure 5f; $P < 0.05$). The ratios of Viola/Anth (Figure 5g) and Viola/Zea (Figure 5h) showed a similar trend and considerably reduced with increasing CO₂ levels ($P < 0.05$). Viola/Zea revealed a significant negative correlation ($P < 0.01$) with increasing CO₂ levels. Alloxanthin (Allo) the marker pigment of cryptophytes and Allo/Chl *a* ratios showed statistically insignificant ($t = 0.95$, $df = 7$, $P > 0.1$) relation with the CO₂ levels. Prasinophytes are usually denoted by the pigment prasinonanthin (Pras) and are a subgroup under the division chlorophyta. They are usually detected in flow cytometry as pico-eukaryotes. In the present experiment Pras/Chl *a* ratios decreased significantly ($t = 2.54$, $df = 7$, $P < 0.05$) in the high CO₂ treated cells, indicating their reduced abundance (figure not shown here).

Flow cytometry analysis

Flow cytometry analysis revealed the presence of *Synechococcus*, heterotrophic bacteria and pico-eukaryotes in the experimental samples. *Prochlorococcus* was not detected. *Synechococcus* cell abundance (varying between 2.19×10^4 and 4.39×10^4 cells ml⁻¹) decreased in the high CO₂ treatments compared to the controls (Figure 6a; $t = 3.53$, $n = 27$, $P < 0.002$). The abundance of pico-eukaryotes (varying from 1.85×10^4 to 3.3×10^4 cells ml⁻¹) was significantly lower in the controls relative to the high CO₂ treatments (Figure 6b; $t = 3.53$, $df = 25$, $P < 0.001$). Flow cytometry analysis revealed that heterotrophic bacterial abundance (varying from 3.45×10^5 to 5.36×10^5 cells ml⁻¹) increased linearly in response to increasing CO₂ levels (Figure 6c) and showed a significant linear positive correlation ($P > 0.01$).

Discussions

$\delta^{13}C_{POM}$, $\delta^{15}N_{POM}$ and evidence of carbon concentration mechanism operation

In the untreated controls, net increase in POC and C : N ratios indicated that a substantial amount of DIC was converted to POM. From the control treatment, slightly depleted values of $\delta^{13}C_{POM}$ in the post-incubation samples indicate the possibility of bicarbonate ions uptake as a

major source of DIC. Since, bicarbonate uptake contributes to low discrimination of ^{13}C ($\delta^{13}\text{C} \approx 0\text{‰}$) compared to the diffusive CO_2 uptake ($\delta^{13}\text{C} \approx -8\text{‰}$)²¹ it is indicated by unaltered or slightly modified values of $\delta^{13}\text{C}_{\text{POM}}$ after incubation under the low CO_2 levels²². Dissolved CO_2 concentration in seawater is $<1\%$ of total DIC and the half-saturation constant (CO_2) of Rubisco (carbon-fixing enzyme) is significantly higher than that²³, and thus can limit the rate of carbon fixation in marine phytoplankton²⁴. In order to fix carbon efficiently under low CO_2 levels, bicarbonate ion is consumed by most of the marine microalgae (the predominant form of DIC in the marine waters) through an active carbon concentration mechanism (CCM) at the cost of energy and which is then

converted to CO_2 with the help of the enzyme carbonic anhydrase²⁵ and has been well documented in marine phytoplankton^{26–28}.

Moreover, CCM requires substantial energy to maintain steady photosynthetic rate under low CO_2 levels and thus, a bigger part of cellular energy is being spent to build bicarbonate transporter proteins, enzymes, etc. involved in CCM operation. Hence, enhanced CCM activity may affect nitrogen utilization efficiency and nitrogen demand can be higher in order to build-up Rubisco and CCM components²⁹. Net DIN uptake and $\delta^{15}\text{N}_{\text{POM}}$ values collectively suggest that nitrogen utilization was comparatively higher in the controls than that of high CO_2 levels and this could be related to the building of CCM components. Thus, it is likely that the phytoplankton community was able to produce significant amount of organic biomass using bicarbonate ions under the control treatments.

$\delta^{13}\text{C}_{\text{POM}}$ values of high CO_2 incubated cells showed depleted values relative to the initial samples and could be due to higher diffusive influx of CO_2 when external CO_2 concentration increases. A reverse relation between dissolved CO_2 and $\delta^{13}\text{C}_{\text{POM}}$ has been reported from *in situ* observations^{30,31}. It has been presumed that upon the increase of external CO_2 concentration, marine phytoplankton may benefit by increased diffusive influx of CO_2 as well as by down regulating CCM and hence can grow faster³². Nonetheless, biomass production was not enhanced in response to higher CO_2 uptake and a similar result has also been observed in other studies^{33,34}. There are field experiments suggesting that some phytoplankton groups may have a constitutive CCM²⁶ and thus increased dissolved CO_2 levels may not benefit photosynthesis and biomass production for those groups.

Dissolved organic carbon leaching in relation to increased heterotrophic bacterial growth and dissolved organic carbon

For the present experiment unaffected biomass build-up in relation to enhanced CO_2 levels could also be due to the alternation in DOC/POC fractionation. Phytoplankton can also increase organic carbon production in response to increasing CO_2 levels and before converting it to macromolecule or POM, it can be leached out from the cell as DOC and may not be reflected in the biomass. It has been observed that under the increased CO_2 levels, DOC production could be higher relative to POC production^{35,36}. However, as has been mentioned earlier, the DOC concentration remains almost unaffected and that could be due to simultaneous consumption of DOC by heterotrophic bacteria. Higher heterotrophic bacterial abundance with increasing CO_2 levels indicates the possibility of higher labile fraction of organic carbon release. It is likely that the rate of organic carbon production was

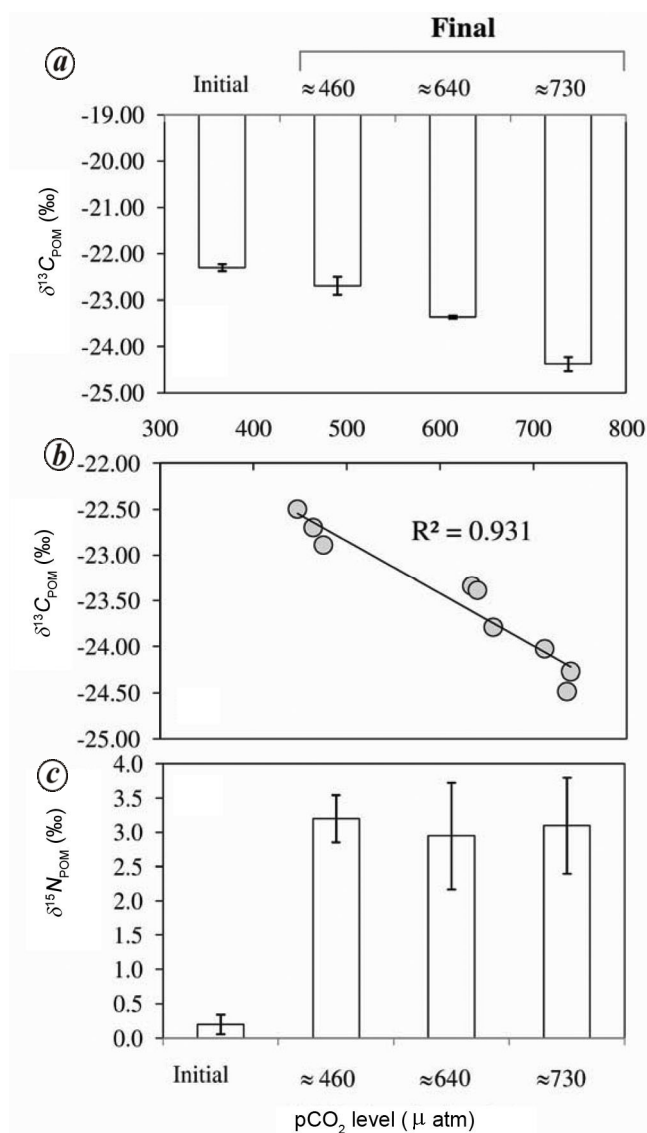


Figure 4. *a*, Initial and final day values of $\delta^{13}\text{C}$ of POM from different CO_2 treatments during the experimental period. *b*, Correlation between final day values of $\delta^{13}\text{C}$ of POM and initial CO_2 levels during the experimental period. *c*, Initial and final day values of $\delta^{15}\text{N}$ of POM from different CO_2 treatments during the experimental period (average \pm SD, $n = 3$).

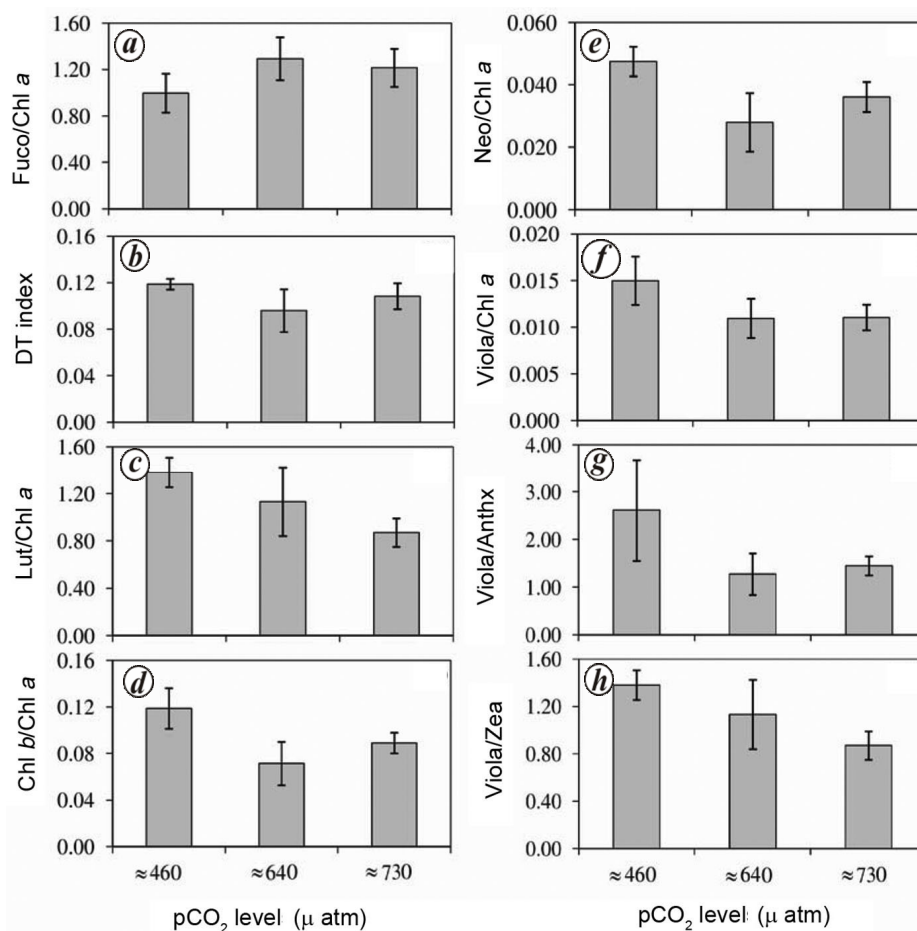


Figure 5. The ratios ($\mu\text{g} : \mu\text{g}$) of (a) Fuco/Chl a (b) DT/(DT + DD), (c) Lut/Chl a, (d) Chl b/Chl a, (e) Neo/Chl a, (f) Viola/Chl a, (g) Viola/Anth and (h) Viol/Zea under different CO₂ levels over the experimental range (average \pm SD, $n = 3$).

probably enhanced under the elevated CO₂ levels and perhaps a significant amount was leached out and simultaneously consumed by heterotrophic bacterial community, and was also observed in an earlier study⁸.

The values of net POC + DOC build-up and DIC uptake were close in the case of control with only 2.13% deviation. Interestingly, the same parameters revealed significant deviation with DIC uptake values (Table 2; almost >22% deviation) in the high CO₂ treatments. It is likely that at the elevated CO₂ levels due to the availability of more labile organic carbon, heterotrophic respiration increased, which might have contributed some amount of CO₂ to the DIC pool. Hence, DIC values were higher than expected and shadowed the original uptake rate. Moreover, if heterotrophic bacteria would respire on the particulate fraction of organic carbon, $\delta^{13}\text{C}_{\text{POM}}$ values would have been enriched instead of being depleted. Considering all these facts together, it is likely that organic carbon production probably increased under the high CO₂ levels. However, it was not converted to POM and was perhaps leached out as DOC, which was further consumed by heterotrophic bacteria.

Phytoplankton community and light stress

Increased Fuco/Chl a ratios under the elevated CO₂ levels may not be due to higher abundance of diatoms. Increased proliferation of diatoms would show higher Si uptake, and net silicate uptake and Si:P uptake ratio did not show any concomitant enhancement in response to increasing CO₂ levels. Presumably, it could be due to enhanced light harvesting pigment (Fuco) synthesis under high CO₂ levels and has been observed in other studies as well (Biswas *et al.*, unpublished data). HPLC pigment analysis revealed that the phytoplankton community expressed the signal of light stress. Phytoplankton groups in the coastal and marine environment, including diatoms, dinophytes and haptophytes possess a xanthophyll cycle under light stress, where they convert DD to DT (by a single de-epoxidation step)³⁷ and thus dissipate the extra energy as heat (non-photochemical quenching; NPQ). Higher DT indexes in the untreated controls relative to the high CO₂ treated cells suggest that the need of NPQ was higher under low CO₂ treatment. Utilization of light energy depends on the availability of sufficient DIC at

the site of carboxylation when other resources are optimum. Hence, under saturated light and low CO₂ levels the absorbed light energy could be in excess relative to its utilization in photosynthesis resulting in net accumulation of unutilized, energy, which may cause photo-damage. Under such conditions, higher amount DD should be converted to DT to dissipate the extra energy resulting in high DT index. On the other hand, increased external CO₂ concentration followed by increasing CO₂ influx inside the cell (as indicated by the $\delta^{13}\text{C}_{\text{POM}}$ data) enhance the substrate availability for Rubisco enabling the cells to utilize greater portion of the absorbed light energy and hence low DT index. Similarly, in other studies, marine diatoms have been shown to better counteract light stress under higher CO₂ levels^{38,39}, mostly due to the availability of more substrate from the Kelvin cycle.

For green algae, a xanthophyll cycle is mainly driven by Viol, where the conversions of the epoxide Viol into de-epoxy containing form Zea through Anth takes place⁴⁰. Decreased ratios of Viol/Chl *a*, Viol/Anth and Viol/Zea with respect to the increasing CO₂ levels indicate that the magnitudes of light stress in the members of Chlorophyta were higher under the elevated CO₂ levels

relative to the control. Higher levels of light stress under low pH have been noticed in green algae⁴¹. Presumably, the sensitivity of diatoms from the study area can be less to increasing CO₂ levels compared to the members of chlorophyta, pico-eukaryotes and prasinophytes. This can be directly linked to the sensitivity of their CCM components and carbon metabolism pathways. In a recent CO₂ perturbation experiment in the Arctic waters⁹, the abundance of prasinophytes showed a positive correlation with the CO₂ levels. However, this trend also varied over different phases of the same experiment. Similar trend was also observed in other large-scale CO₂ enrichment experiments¹¹. This difference could be explained by the existence of different modes of CCM operation in these groups of microalgae, which can even vary in the species level.

Conclusion

The present study shows some basic facts about the responses of the phytoplankton community to short-term CO₂ enhancement from the Yellow Sea coastal waters. The results reveal the differential responses of diverse microalgal groups to increased CO₂ levels. Presumably, the diatom-dominated phytoplankton community can utilize bicarbonate ion under low CO₂ levels. However, higher diffusive influx of CO₂ may not result in higher biomass production in this phytoplankton community, and might impact POC/DOC partitioning in marine phytoplankton in this area. This may further accelerate heterotrophic bacterial activity and hence the carbon dynamics. Further investigations on a longer timescale would provide better insight about the same.

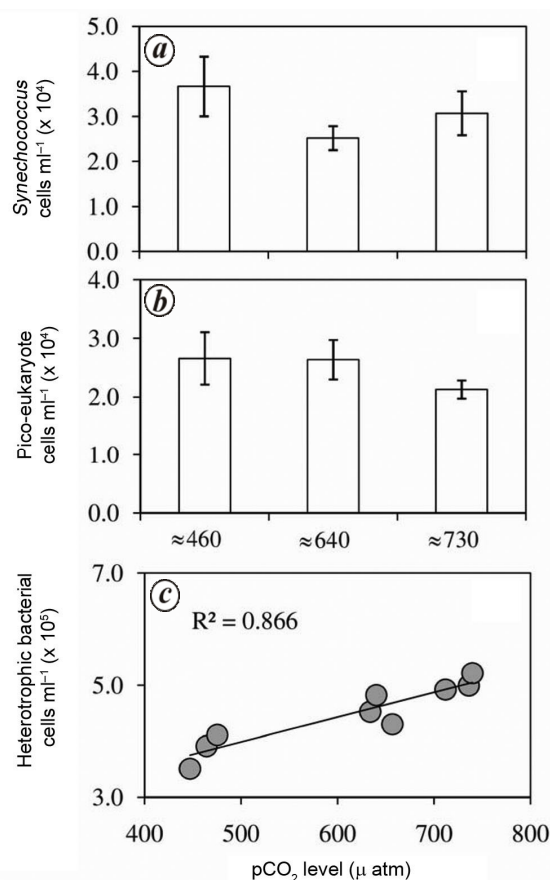


Figure 6. Final day flow-cytometric cell counts of (a) *Synechococcus*, (b) pico-eukaryotes and (c) heterotrophic bacteria under different CO₂ levels over the experiment range (average \pm SD, $n = 6-9$).

1. Sabine, C. L. and Tanhua, T., Estimation of anthropogenic CO₂ inventories in the ocean. *Annu. Rev. Mar. Sci.*, 2010, **2**, 175–198.
2. Doney, S. C., Fabry, V. J., Feely, R. A. and Kleypas, J. A., Ocean acidification, the other CO₂ problem. *Annu. Rev. Mar. Sci.*, 2009, **1**, 169–192.
3. Raven, J. *et al.*, *Ocean Acidification due to Increasing Atmospheric Carbon Dioxide*, The Royal Society London UK, 2005.
4. Boyd, P. W., Strzepek, Fu, F. and Hutchins, D. A., Environmental control of open-ocean phytoplankton groups, now and in the future. *Limnol. Oceanogr.*, 2010, **55**(3), 1353–1376.
5. Beardall, J., Stojkovic, S. and Larsen, S., Living in a high CO₂ world, impacts of global climate change on marine phytoplankton. *Plant Ecol. Divers.*, 2009, **2**(2), 191–205.
6. Collins, S., Rost, B. and Rynearson, T. A., Evolutionary potential of marine phytoplankton under ocean acidification. *Evol. Appl.*, 2014; doi: 10.1111/eva.12120.
7. Hein, M. and Sand-Jensen, K., CO₂ increases oceanic primary production. *Nature*, 1997, **388**, 526–527.
8. Biswas, H., Cros, A., Yadav, K., Ramana, V. V., Prasad, V. R., Acharyya, T. and Babu, P. V., The response of a natural phytoplankton community from the Godavari River Estuary to increasing CO₂ concentrations during the pre-monsoon period. *J. Exp. Mar. Biol. Ecol.*, 2011, **407**, 284–293.
9. Schulz, K. G. *et al.*, Temporal biomass dynamics of an Arctic plankton bloom in response to increasing levels of atmospheric carbon dioxide. *Biogeosciences*, 2013, **10**, 161–180.

10. Meakin, N. G. and Wyman, M., Rapid shifts in picoeukaryote community structure in response to ocean acidification. *ISME J.*, 2011, **5**, 1397–1405.
11. Feng, Y. *et al.*, Effects of increased pCO₂ and temperature on the North Atlantic spring bloom, I. The phytoplankton community and biogeochemical response. *Mar. Ecol. Prog. Ser.*, 2009, **388**, 13–25.
12. Rost, B., Zondervan, I. and Wolf-Gladrow, D., Sensitivity of phytoplankton to future changes in ocean carbonate chemistry, Current knowledge contradictions and research directions. *Mar. Ecol. Prog. Ser.*, 2008, **373**, 227–237.
13. Lewis, E. and Wallace, D. W. R., CO₂SY_S_calc_DOS_Original, program developed for CO₂ system calculations ORNL/CDIAC-105 carbon Dioxide Information Analysis Center Oak Ridge National Laboratory US Department of Energy, 1998, Oak Ridge, Tennessee.
14. Riebesell, U., Fabry, V. J., Hansson, L. and Gattuso, J.-P. (eds), *Guide to Best Practices for Ocean Acidification Research and Data Reporting*, Luxembourg, Publications Office of the European Union, 2010, p. 260.
15. Dickson, A. G., Afghan, J. D. and Anderson, G. C., Reference materials for oceanic CO₂ analysis. A method for the certification of total alkalinity. *Mar. Chem.*, 2003, **80**, 185–385.
16. Parsons, T. R., Maita, Y. and Lalli, C. M., *A Manual of Chemical and Biological Methods for Seawater Analysis*, Pergamon, Oxford, 1984, p. 173.
17. Grasshoff, K., Kremling, K. and Ehrhardt, M., In *Methods of Seawater Analysis* (ed. Grasshoff, K.), Weinheim Federal Republic of Germany, WILEY-VCH Verlag GmbH, 1999.
18. Zapata, M. and Garrido, J. L., Influence of injection conditions in reversed-phase high-performance liquid chromatography of chlorophylls and carotenoids. *Chromatography*, 1991, **31**, 589–594.
19. Zapata, M., Rodríguez, F. and Garrido, J. L., Separation of chlorophylls and carotenoids from marine phytoplankton. A new HPLC method using a reversed phase C8 column and pyridine-containing mobile phases. *Mar. Ecol. Prog. Ser.*, 2000, **195**, 29–45.
20. Aspila, K. I., Agemian, H. and Chau, A. S. Y., A semi automated method for the determination of inorganic organic and total phosphate in sediments. *Analyst*, 1976, **101**, 187–197.
21. Mook, W. G., Bommerson, J. C. and Staverman, W. H., Carbon isotope fractionation between dissolved bicarbonate and gaseous carbon dioxide. *Earth Planet. Sci. Lett.*, 1974, **22**(2), 169–176.
22. Giordano, M., Beardall, J. and Raven, J. A., CO₂ concentration mechanisms in algae, mechanisms, environmental modulation and evolution. *Annu. Rev. Plant Biol.*, 2005, **56**, 99–131.
23. Badger, M. *et al.*, The diversity and coevolution of Rubisco plastids, pyrenoids and chloroplast-based CO₂-concentrating mechanisms in algae. *Can. J. Bot.*, 1998, **76**(6), 1052–1071.
24. Riebesell, U., Wolf-Gladrow, D. A. and Smetacek, V., Carbon dioxide limitation of marine phytoplankton growth rates. *Nature*, 1993, **361**, 249–251.
25. Morel, F. M. M., Reinfelder, J. R., Roberts, S. B., Chamberlain, C. P., Lee, J. G. and Yee, D., Zinc and carbon co-limitation of marine phytoplankton. *Nature*, 1994, **369**, 740–742.
26. Cassar, N., Laws, E. A., Bidigare, R. R. and Popp, B. N., Bicarbonate uptake by Southern Ocean phytoplankton. *Global Biogeochem. Cycles*, 2004, **18**, GB2003; doi: 10.1029/2003GB002116.
27. Tortell, P. D., DiTullio, G. R., Sigman, D. M. and Morel, F. M. M., CO₂ effects on taxonomic composition and nutrient utilization in an Equatorial Pacific phytoplankton assemblage. *Mar. Ecol. Prog. Ser.*, 2002, **236**, 37–43.
28. Burkhardt, S., Amoroso, G., Riebesell, U. and Sültemeyer, D., CO₂ and HCO₃⁻ uptake in marine diatoms acclimated to different CO₂ concentrations. *Limnol. Oceanogr.*, 2001, **46**, 1378–1391.
29. Beardall, J. and Giordano, M., Ecological implications of microalgal and cyanobacterial CO₂ concentrating mechanisms and their regulation. *Funct. Plant Biol.*, 2002, **29**, 335–347.
30. Rau, G. H., Takahashi, T., DesMarais, D. J., Repeta, D. J. and Martin, J. H., The relationship between organic matter δ¹³C and CO_{2(aq)} in ocean surface waters; data from a JGOFS site in the Northeast Atlantic Ocean and a model. *Geochim. Cosmochim. Acta*, 1992, **56**, 1413–1419.
31. Rau, G. H., Chavez, F. P. and Friederich, G. E., Plankton ¹³C/¹²C variations in Monterey Bay, California: evidence of non-diffusive inorganic carbon uptake by phytoplankton in an upwelling environment. *Deep Sea Res. Part 1*, 2011, **48**, 79–94.
32. Reinfelder, J. R., Carbon concentrating mechanisms in eukaryotic marine phytoplankton. *Annu. Rev. Mar. Sci.*, 2011, **3**, 291–315.
33. Schulz, K. G. *et al.*, Build-up and decline of organic matter during PeECE III. *Biogeosciences*, 2008, **5**, 707–718.
34. Yoshimura, T., Nishioka, J. K., Suzuki, H., Kiyosawa, H. H. and Watanabe, Y. W., Impacts of elevated CO₂ on phytoplankton community composition and organic carbon dynamics in nutrient-depleted Okhotsk Sea surface waters. *Biogeosci. Discuss*, 2009, **6**, 4143–4163.
35. Engel, A. *et al.*, Transparent exopolymer particles and dissolved organic carbon production by *Emiliania huxleyi* exposed to different CO₂ concentrations; a mesocosm experiment. *Aquat. Microb. Ecol.*, 2004, **34**, 93–104.
36. Kim, J. H., Lee, K., Shin, K., Yang, E. J., Engel, A., Karl, D. and Kim, H. C., Shifts biogenic carbon flow from particulate to dissolved forms under high carbon dioxide and warm ocean conditions. *Geophys. Res. Lett.*, 2011, **38**, L08612; doi:10.1029/2011GL047346.
37. Lavaud, J., Van Gorkom, H. and Etienne, A. L., Influence of the diadinoxanthin pool size on photoprotection in the marine planktonic diatom *Phaeodactylum tricoratum*. *Plant Physiol.*, 2002, **129**, 1398–1406.
38. Li, Y., Gao, K., Villafane, V. E. and Helbling, E. W., Ocean acidification mediates photosynthetic response to UV radiation and temperature increase in the diatom *Phaeodactylum tricoratum*. *Biogeosciences*, 2012, **9**, 3931–3942.
39. Chen, H., Guan, W., Zeng, G., Li, P. and Chen, S., Alleviation of solar ultraviolet radiation (UVR)-induced photoinhibition in diatom *Chaetoceros curvisetus* by ocean acidification. *J. Mar. Biol. Assoc. UK*, 2014; doi: <http://dx.doi.org/10.1017/S0025315414001568>.
40. Dimier, C., Giovanni, S., Ferdinando, T. and Brunet, C., Comparative ecophysiology of the xanthophyll cycle in six marine phytoplanktonic species. *Protist*, 2009, **160**(3), 397–411.
41. Sobrino, C., Neale, P. J. and Lubian, L. M., Interaction of UV radiation and inorganic carbon supply in the inhibition of photosynthesis. Spectral and temporal responses of two marine picoplankters. *Photochem Photobiol.*, 2005, **81**, 384–393.

ACKNOWLEDGEMENTS. NIO Contribution number is 5682. This study was jointly funded by the collaborative project of National Science Foundation (NSF Contract No. 40910212) China and CSIR, India. We thank the Director, National Institute of Oceanography (NIO), Goa and Scientist-in-Charge, Regional Centre, NIO, Visakhapatnam for support and approval for this opportunity to work with the Chinese Scientists. We also thank Drs Dileep Kumar and P. C. Rao (NIO, Goa) for conducting this India–China collaborative programme. Prof. Guling Zhang and Jing Ling Ren (Ocean University of China, Qingdao) for their active co-operation and kind support for conducting this work and Zhao Min, Yu-Chuan Zhao and Guo-Dong Song (Ocean University of China, Qingdao) are acknowledged for their kind help.

Received 14 July 2014; revised accepted 28 November 2014